International Journal of Current Engineering and Technology
E-ISSN 2277 – 4106, P-ISSN 2347 – 5161
Available at http://inpressco.com/category/ijcet


*Research Article*

# Performance Evaluation of Solar Air Collector in Sensible Heat Storage by Forced Convection with Cherry Powder

**Thakar Mihirkumar J[#*] and Prajapati Dhaval K^**

[#]Dairy engineering, G. N. Patel College of Dairy Technology, Sardar Dantiwada Agricultural University, S. K. Nagar, Gujarat, India
^Hansaba College of Engineering and Technology, Siddhpur, Gujarat, India

Received 11 Nov 2019, Accepted 13 Jan 2020, Available online 17 Jan 2020, **Vol.10, No.1 (Jan/Feb 2020)**


### *Abstract*

*In practice different kinds of solar air heaters are available for domestic heating and industrial air heating purposes, space heating, process heating and agricultural applications. Advantage of this system is to use of renewable energy source that is free in cost and an eco-friendly, economical and simple device. There are so many researcher who focuses to improve the efficiency and to maintain the continuous heat supply of the double pass solar air heater using sensible storage material. The heat transfer and friction characteristics due to the sensible storage material of solar air heaters have been reviewed in this research. A double pass solar air heater was fabricated and integrated with thermal storage system and powdered cherry pits are used as a thermal storage medium. The performance of this heater was studied for different configurations. The solar heater integrated with thermal storage delivered comparatively high temperature. The efficiency of the air heater integrated with thermal storage was also higher than the air heater without thermal storage system. The study concluded that the presence of the thermal storage medium at the absorber plate is the best configuration.*


***Keywords:*** *Cherry pits powder, Double pass solar air heater, Solar Absorber plates, Sensible heat storage system*

## 1. Introduction

Energy in various forms has played an important role in worldwide industrial progress and economics. Energy crisis and global warming was lead to find an alternative way to overcome the above worsening situation. Renewable energy plays a major solution and thereby meets our energy demand and reduces the CO2 emission which reduces the greenhouse effect. And also reduce fossil fuel. In the renewable energy side, Sun is the mother for all sources and harnessing the solar energy in proper ways can eliminate the energy crisis of the world. This freely available solar radiation is infinite, non-polluting resource of solar energy. The easiest way to use solar energy is to convert it into thermal energy by using solar air heaters. Among different types of solar thermal systems, solar air heaters are widely used systems due to lower cost and simplicity in design. Direct as well as diffused solar radiations are absorbed at the absorber plate and transferred to the air that flows through the passage underneath the absorbing surface. The thermal efficiency of solar air heaters is depending on the useful heat gain by the collector fluid. As the value of heat transfer coefficient for air is low. Which reduces the heat transfer rate and thus increases the heat loss to the surroundings and decrease the efficiency of solar air heater? It is believed that the formation of laminar viscous sub-layer over the heated surface offers thermal resistance to heat transfer. To breaking the boundary sub layer by providing the artificial roughness improve the heat transfer rate.

## 2. Major parts of Solar air heater & its role

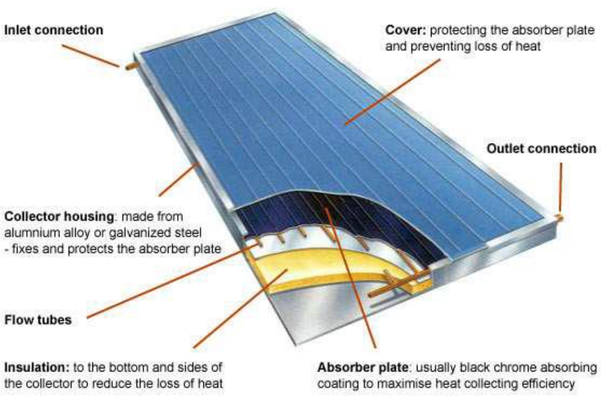


Collector - A typical solar air heating collector is made up of wood, galvanized iron sheet, or concrete. Inner

*Corresponding author's ORCID ID: 0000-0001-7703-8750
DOI: https://doi.org/10.14741/ijcet/v.10.1.5

surface is blackened coating to absorb the maximum solar radiation during the day period. Inclination is provided to receive maximum solar radiation.

Glass cover - Glass is put on the top for allowing the maximum solar radiation inside the solar air collector, to minimize convective heat loss from absorber plate.

Absorber Plate- Main element of solar air heater. And absorb the maximum possible amount of solar radiation.

Insulation - Outer side walls is insulated with different insulation materials such as puff, thermocol, wood, fiber, glass wool, etc.

Basic type of solar air heater

1. Passive Type -In this type of solar air heater is simple in manufacturing and easy to maintenance. This types of techniques include designing space according to natural circulation not require external sources.
2. Active Type- In this type of solar air heater external power sources (fan, blower etc.) are provided for forced convection or to heat the air. These types of solar air heaters are consume an electricity or external power.

## 3. Method

Whole Experimental setup will made from galvanized iron sheet/ mild steel sheet of 1.5mm. The side walls of the solar air heater will be covered with the help of puff / glass wool insulation. Experimental setup will design with the help of software and developed as per our requirements in it. Absorber plate and absorber material will be defined and implement in the experimental setup. All the sides and absorber plate surfaces were painted with black paint to absorb maximum solar radiation during the day. Axial fan/blower with control valve was fitted to forced circulation and controlling of air flow. All the data will be measured in the sunny days. Results will be measured with the help of measuring instruments such as solar radiation meter (pyranometer), Temperature indicator, thermocouple, and manometer. Mathematical calculations determine for find out the efficiency of the double pass solar air heater.

### *3.1Experimental setup & working of solar air heater*

#### *3.1.1 Thermal analysis*

The theoretical model employed for the study of the solar collector that operates in unsteady state is made using a thermal energy balance.

[Accumulated energy] + [Energy gain] = [Absorbed energy] + [Lost energy] (3.1)

For each term of Eq. (3.1) the following expressions are formulated

Accumulated Energy $= MpCp\ (dTp, avg|dt)$ (3.2)

Energy Gain$=$ $mp\ cp\ (Tout\ - Tin)$ (3.3)

Absorbed Energy $= \eta o\ L\ Ac$ (3.4)

Lost Energy$=$ $Uc(Tp, avg - To)\ Ac$ (3.5)

By combining Eq. (3.2) to (3.5), the thermal energy balance equation necessary to describe the solar collector functioning is obtained:

$$MpCp(dTp, avg|dt) + mp\ cp\ (Tout\ - Tin) = \eta o\ L\ A\ c + Uc(Tp, avg - To)\ Ac \quad (3.6)$$

The optical yield ($\eta o$) and the energy lose coefficient ($U$) are the parameters that characterize the behavior of the solar collector. Note that $\eta o$ represents the fraction of the solar radiation absorbed by the plate and depends mainly on transmittance of the transparent covers and on the absorbance of the plate. The energy loss coefficient includes the losses by the upper cover, the laterals, and the bottom of the collector. The upper cover losses prevail over the others, depending to a large extent on the temperature nd emissivity of the absorbent bed, and besides, on the convective effect of the wind on the upper cover. The thermal efficiency of the solar collectors ($\eta o$) is defined as the ratio between the energy gain and the solar radiation incident on the collector plane:

$$n = mp\ cp(Tout\ - Tin) / \text{L Ac} \quad (3.7)$$

Equation for mass flow rate is,

$$m = \rho\ Ac\ v \quad (3.8)$$

#### *3.1.2 Thermo-hydraulic behavior of flow inside solar heater duct*

The application of artificial roughness on the underside of the absorber plate of solar heater duct brings out significant changes in fluid flow behavior adjacent to the plate surface. It is believed that the change in the fluid flow pattern in the vicinity of heated wall has notable effect on heat transfer rates and skin friction. The literature pertaining to flow through roughened solar air heater duct reveals that the protrusions in the form of repeated ribs cause flow separations and reattachments at multiple locations which tends to enhance the local wall turbulence and thereby leads to higher heat transfer coefficient at some localized spots. The simultaneous rise in heat transfer and pressure drop creates a misleading situation where it becomes difficult to identify the actual gain as a result of the application of artificial roughness. In order to evaluate the net improvement in the performance of solar heater by considering artificially roughened duct, the coexisting thermal and hydraulic effects are to be examined relative to each other. Performance parameter that shows relative value of thermal gain than that of hydraulic loss, called thermo-hydraulic performance parameter, expressed as:

$$\eta = {(Nur|Nux)}\Big/{(fr|fx)^{1/3}} \quad (3.9)$$

This factor shows the enhancement of heat transfer due to application of roughness over the smooth surface for the same pumping power requirements. The consideration of hydraulic performance in a flow through solar air heater duct is important as the blower consumes mechanical power to impart the flow energy to the air and is sensitive to the change in pressure drop across the duct. The Nusselt number for roughened surface (Nur) can be estimated by using the mean heat transfer coefficient (h) as:

$$Nur = \frac{h\,d}{k} \quad (3.10)$$

The Nusselt number for smooth duct can be obtained by using the Dittus-Boelter Equation given as:

$$Nus = 0.23\, Re^{0.8} Pr^{0.4} \quad (3.11)$$

The pressure drop for fully developed turbulent flow through roughened duct is obtained by friction factor (fr) as:

$$fr = \frac{2\,(\Delta p|l)D}{\rho v^2} \quad (3.12)$$

The frictional losses in a smooth duct in terms of friction factor are given by the Modified Blasius Equation as:

$$fs = 0.085 Re^{-0.25} \quad (3.13)$$

The thermal performance of solar air heater is depending on the useful heat gain by collector fluid which in turn is a strong function of Nusselt number. The Nusselt number varies with the change in the values of fin parameters and flow Reynolds number. The effect of Reynolds number on the average Nusselt number over the absorber plate surface for different fin geometries. It can be noticed that the Nusselt number increases with the increase in Reynolds number in all cases. The Nusselt number pertinent to Multi shaped fin with gap approached to the maximum value at among all the roughness geometries irrespective of the value of Reynolds number. At low Reynolds number (Re: 4000).

*3.1.3 Exergy analysis*

This article focuses on the combination of the two laws of thermodynamics, which are described in the concept of exergy analysis. The assumptions made in the analysis presented in this study are:

a) Steady state, steady flow operation,
b) Negligible potential and kinetic energy effects and no chemical or nuclear reactions,
c) Air is an ideal gas with a constant specific heat, and its humidity content is ignored,
d) The directions of heat transfer to the system and work transfer from the system are positive.

The mass balance equation can be expressed in the rate form as

$$\sum m_{in} = \sum m_{out} \quad (3.14)$$

Where $m$ is the mass flow rate, and the subscript in stands for inlet and out for outlet.

If the effects due to the kinetic and potential energy changes are neglected, the general energy and exergy balances can be expressed in rate form as given below:

$$\sum E_{in} = \sum E_{out} \quad (3.15)$$

$$\sum E_{in} - \sum E_{out} = \sum E_{dest} \quad (3.16)$$

$$\sum Ex_{heat} - \sum Ex_{work} + \sum Ex_{mass,in} - \sum Ex_{mass,out} = \sum E_{dest} \quad (3.17)$$

Using Eq. (3.14), the rate form of the general exergy balance can also be written as

$$\sum\left(1 - \frac{Te}{Ts}\right) Qs - W + \sum m_{in}\ \Psi_{in} - \sum m_{out}\ \Psi_{out} = Ex, dest \quad (3.18)$$

Where,

$$\Psi in = (h_{in} - h_e) - Te\,(s_{in} - s_e) \quad (3.19)$$

$$\Psi out = (h_{out} - h_e) - Te\,(s_{out} - s_e) \quad (3.20)$$

If Eq. ((3.15) and (3.16) are substituted in Eq. (3.17), it is arranged that

$$\left(1 - \frac{Te}{Ts}\right) Qs - m[(hout - hin) - Te\,(Sout - Sin)] = Ex, dest \quad (3.21)$$

Where Qs is solar energy absorbed by the collector absorber surface and it is evaluated by the expression

$$Qs = H\,(\tau\alpha) Ac \quad (3.22)$$

The enthalpy and entropy changes of the air in the collector are expressed by

$$\Delta h = h_{out} - h_{in} = cp\,(T_{f,out} - T_{f,in}) \quad (3.23)$$

$$\Delta S = S_{out} - S_{in} = cp\, ln \left(\frac{T_{f,out}}{T_{f,in}}\right) - Rln \frac{pout}{pin} \quad (3.24)$$

Substituting Eq. (3.23) – (3.24) in Eq. (3.21) it may be rewritten as

$$\left(1-\frac{Te}{Ts}\right)H\,(\tau\alpha)Ac\;-mcp\,(T_{f,out}-T_{f,in})+$$
$$m\;cp\;Te\;ln\left(\frac{T_{f,out}}{T_{f,in}}\right)-\;mRTeln\frac{pout}{pin}\;=\;Ex,dest \quad (3.25)$$

The irreversibility *dest Ex* can be directly evaluated from the following equation

$$Ex_{dest}=Te\;Sgen \quad (3.26)$$

The second law efficiency is calculated as

$$\eta_{II}=1-\frac{T_eS_{gen}}{[1-(T_e/T_S)]Qs} \quad (3.27)$$

All physical properties of air were selected according to the following bulk mean temperature:

$$\Delta Tm=(T_{in}+\;T_{out})/2 \quad (3.28)$$

**Experimental Setup**

The experimental setup will be designed to measure the effect of metallic wiry sponge inserted in the double pass solar air heater. The experimental setup has been fabricated from the galvanized iron sheet of 16” gauge (1.6mm), the reduced draft has been provided to the equally air distribution at the inlet and outlet section. The absorber M.S. plate is put at the middle of the solar air heater and all inner surfaces with absorber plate coated black paint to absorb the maximum solar radiation. Adjustable inclination stand has been designed to measure the effect of different inclination angles of solar air heater. For batter comparison there are two set up will fabricated of same dimensions. Absorber plate area is designed to measure the effect is 0.5m2. Forced draft fan is placed at the inlet of the DPSAH. 4mm clear glass is placed at the top of the air heater to reduce the heat loss.

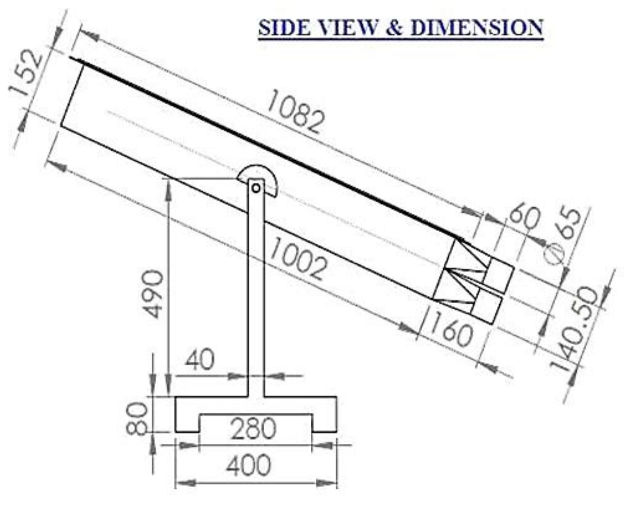


**Figure 1** Experimental Setup CAD Design

**Figure 2** Experimental Setup

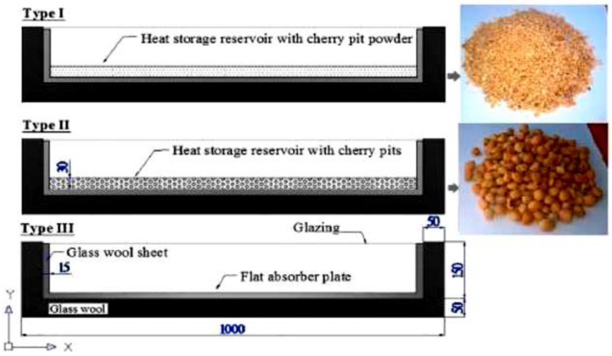


**Figure 3** Experimental Setup Dimensions

**Figure 4** Experimental Setup Arrangement

**Figure 5** Experimental Setup Arrangement

## 4. Result

| Experimental Result at Different Mass Flow Rate on (**without cherry PITS**) | | | | | | | |
|---|---|---|---|---|---|---|---|
| **Time** | **Solar Radiation (I) Watt/m2** | **Mass flow rate (m) Kg/sec** | **Average Temperature of Absorber Plate Tap(oC)** | **Inlet Temp. Ti (oC)** | **Outlet Temp. To (oC)** | **Temp. Difference ΔT=To-Ti (oC)** | **Efficiency = m cpΔt/I*A, cp=1004 kJ/kg.K** |
| 9:00 AM | 594 | 0.0221 | 66.6 | 35 | 58.7 | **23.7** | 0.96702187 |
| 10:00 AM | 719 | 0.0221 | 66.8 | 35.5 | 62.1 | **26.6** | 0.89665865 |
| 11:00 AM | 738 | 0.0221 | 70 | 39.8 | 62.8 | **23** | 0.75534589 |
| 12:00 PM | 829 | 0.0221 | 70.2 | 39.2 | 58.5 | **19.3** | 0.56425728 |
| 1:00 PM | 992 | 0.0221 | 71.4 | 37.4 | 58.8 | **21.4** | 0.52284926 |
| 2:00 PM | 895 | 0.0221 | 72.8 | 39 | 61.9 | **22.9** | 0.62013585 |
| 3:00 PM | 775 | 0.0221 | 71.1 | 37.8 | 63.3 | **25.5** | 0.79746728 |
| 4:00 PM | 675 | 0.0221 | 65.9 | 37.5 | 61.4 | **23.9** | 0.85816050 |
| 5:00 PM | 448 | 0.0221 | 62.2 | 36.9 | 53.9 | **17** | 0.91969813 |
| 6:00 PM | 196 | 0.0221 | 52.3 | 36 | 43 | **7** | 0.86559824 |
| 7:00 PM | 81 | 0.0221 | 43.2 | 34.7 | 36.7 | **2** | 0.59843829 |
| 8:00 PM | | 0.0221 | 35.1 | 32.6 | 32.8 | **0.2** | |
| **Average** | **631.090909** | | **62.3** | **36.783333** | **54.491667** | **17.70833** | **0.7605119** |

The data above are been extracted by using instrument such as digital temperature sensor and pyranometer, with addition to that flow rate is been stabled by using gaming adaptor in which there were different sets of voltage ratings. The data of first day is been taken by considering mass flow rate constant as 0.02211 kg/sec, and without using cherry pits material

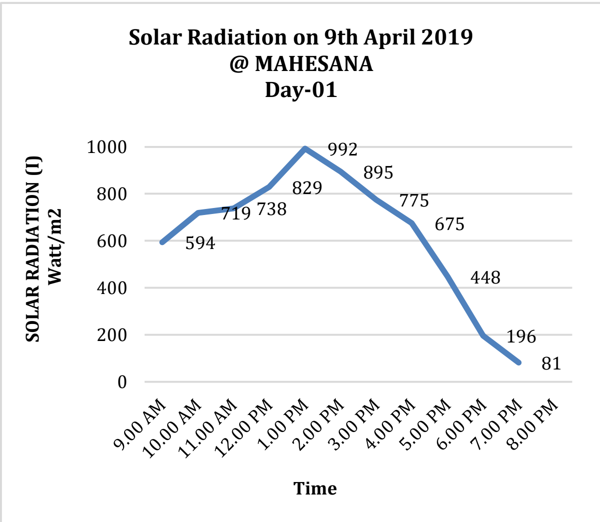


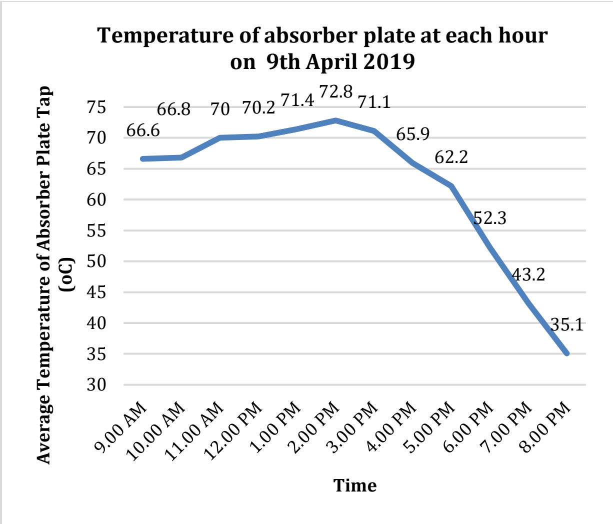


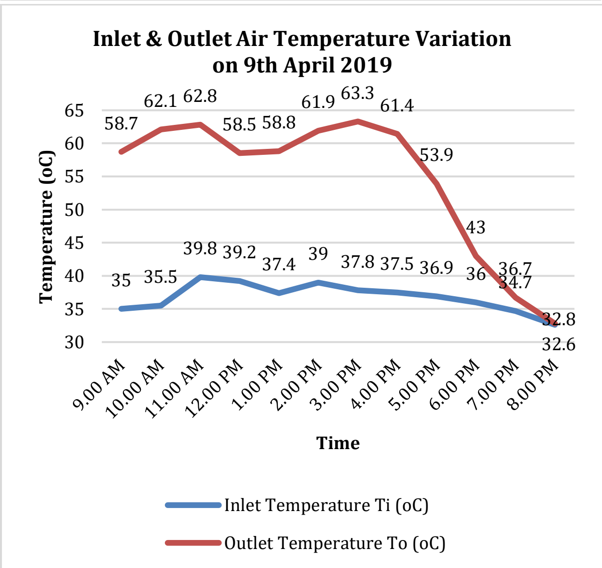


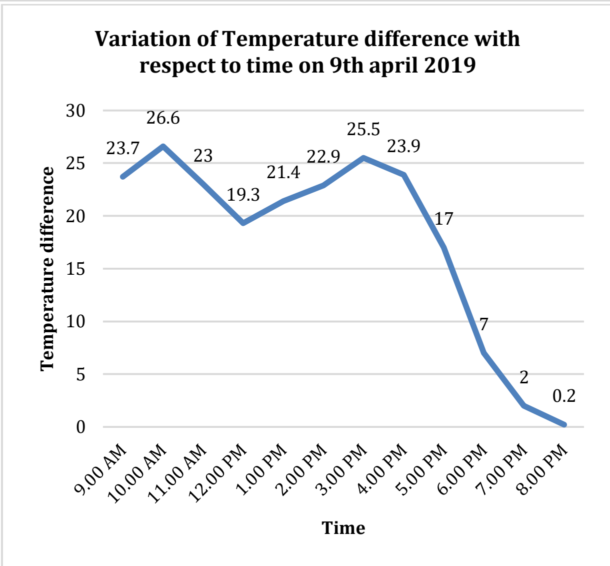

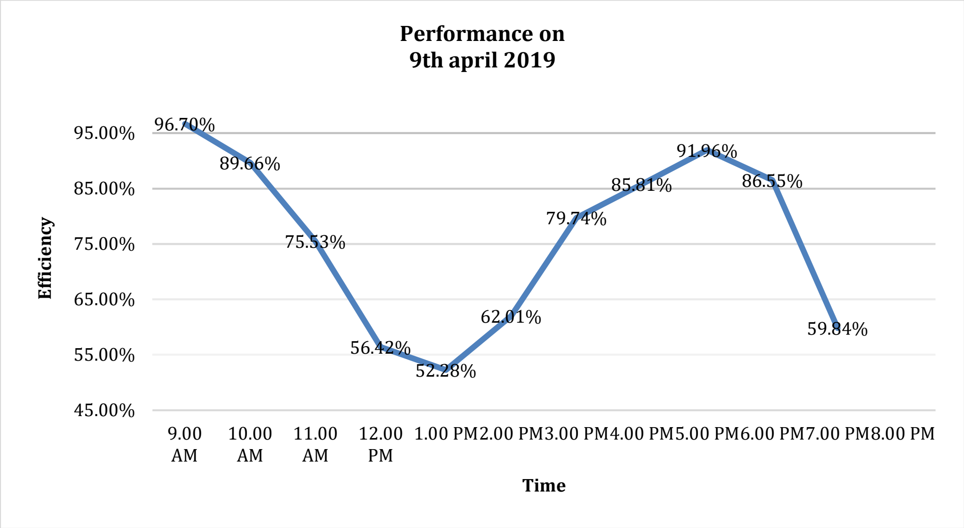
Performance on
9th april 2019
Efficiency
95.00%
85.00%
75.00%
65.00%
55.00%
45.00%
96.70%
89.66%
75.53%
56.42%
52.28%
62.01%
79.74%
85.81%
91.96%
86.55%
59.84%
9.00 AM
10.00 AM
11.00 AM
12.00 PM
1.00 PM
2.00 PM
3.00 PM
4.00 PM
5.00 PM
6.00 PM
7.00 PM
8.00 PM
Time

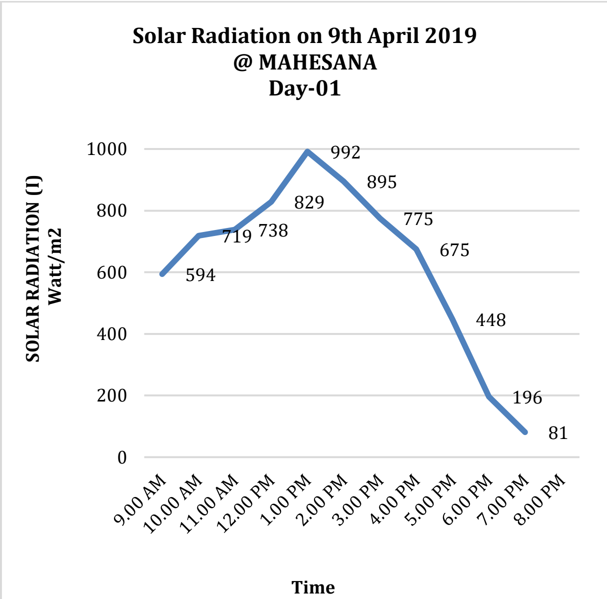
Solar Radiation on 9th April 2019
@ MAHESANA
Day-01
SOLAR RADIATION (I) Watt/m2
1000
800
600
400
200
0
594
719
738
829
992
895
775
675
448
196
81
9.00 AM
10.00 AM
11.00 AM
12.00 PM
1.00 PM
2.00 PM
3.00 PM
4.00 PM
5.00 PM
6.00 PM
7.00 PM
8.00 PM
Time

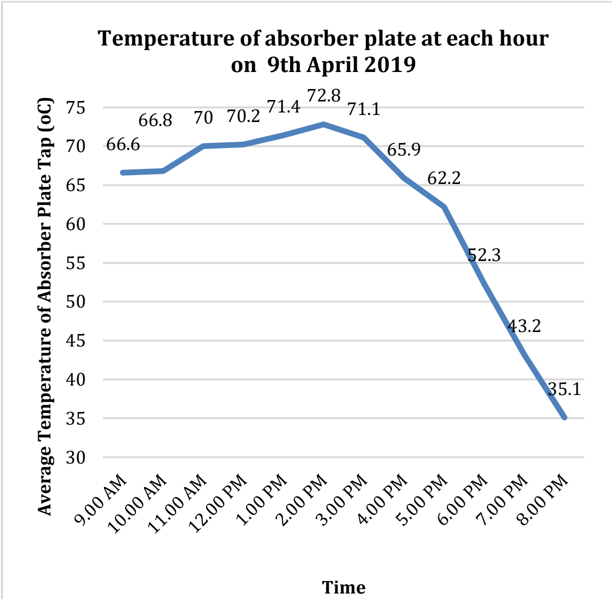
Temperature of absorber plate at each hour
on 9th April 2019
Average Temperature of Absorber Plate Tap (oC)
75
70
65
60
55
50
45
40
35
30
66.6
66.8
70
70.2
71.4
72.8
71.1
65.9
62.2
52.3
43.2
35.1
9.00 AM
10.00 AM
11.00 AM
12.00 PM
1.00 PM
2.00 PM
3.00 PM
4.00 PM
5.00 PM
6.00 PM
7.00 PM
8.00 PM
Time

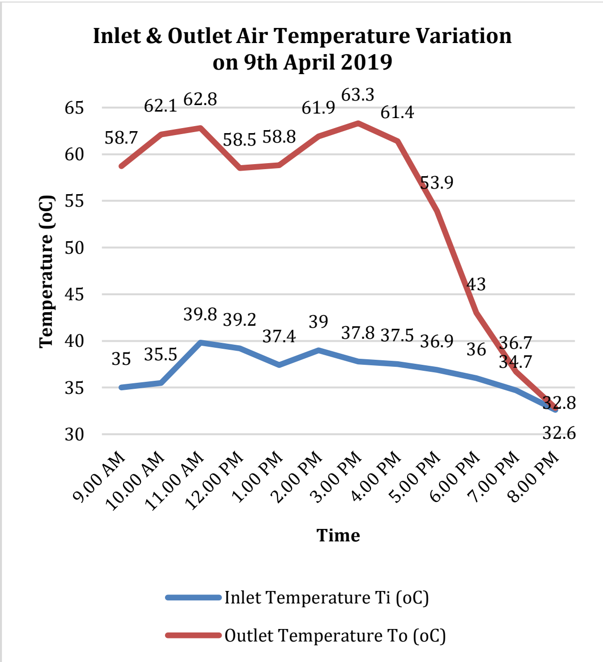
Inlet & Outlet Air Temperature Variation
on 9th April 2019
Temperature (oC)
65
60
55
50
45
40
35
30
58.7
62.1
62.8
58.5
58.8
61.9
63.3
61.4
53.9
43
36.7
32.8
35
35.5
39.8
39.2
37.4
39
37.8
37.5
36.9
36
34.7
32.6
9.00 AM
10.00 AM
11.00 AM
12.00 PM
1.00 PM
2.00 PM
3.00 PM
4.00 PM
5.00 PM
6.00 PM
7.00 PM
8.00 PM
Time
Inlet Temperature Ti (oC)
Outlet Temperature To (oC)

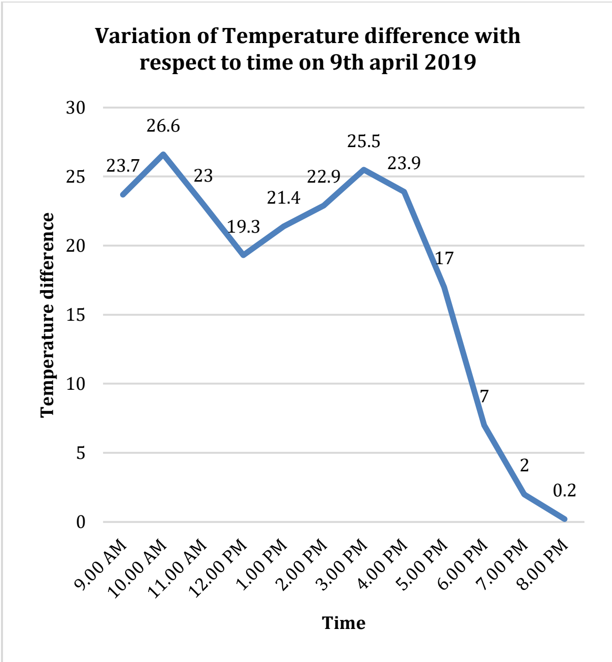
Variation of Temperature difference with
respect to time on 9th april 2019
Temperature difference
30
25
20
15
10
5
0
23.7
26.6
23
19.3
21.4
22.9
25.5
23.9
17
7
2
0.2
9.00 AM
10.00 AM
11.00 AM
12.00 PM
1.00 PM
2.00 PM
3.00 PM
4.00 PM
5.00 PM
6.00 PM
7.00 PM
8.00 PM
Time

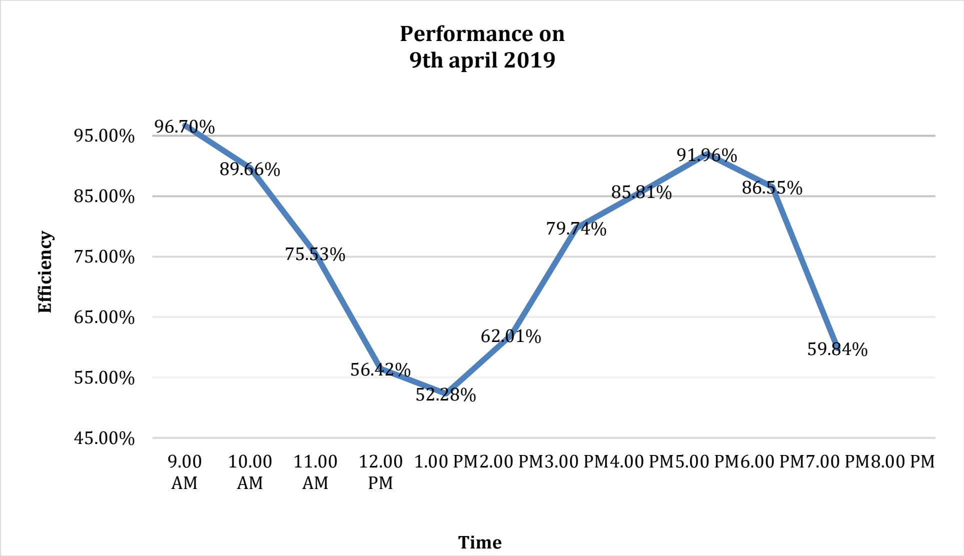


| Experimental result at different mass flow rate on **12th APRIL 2019** @ MAHESANA (LAT: 23.55 , LONG:72.35) **with Cherry pits material** | | | | | | | |
|---|---|---|---|---|---|---|---|
| **Time** | **SOLAR RADIATION (I) Watt/m2** | **Mass flow rate (m) Kg/sec** | **Average Temperature of Absorber Plate Tap (oC)** | **Inlet Temp. Ti (oC)** | **Outlet Temp. To (oC)** | **Temp. Difference ΔT=To-Ti (oC)** | **Efficiency = m cpΔt/I*A, cp=1004 kJ/kg.K** |
| 9:00 AM | 561 | 0.0221 | 66.8 | 35.3 | 54.2 | **18.9** | 0.81653224 |
| 10:00 AM | 723 | 0.0221 | 67.1 | 35.5 | 59.8 | **24.3** | 0.81459618 |
| 11:00 AM | 740 | 0.0221 | 70.8 | 39.6 | 60.8 | **21.2** | 0.69435015 |
| 12:00 PM | 807 | 0.0221 | 63.1 | 39.2 | 58.2 | **19** | 0.57062981 |
| 1:00 PM | 998 | 0.0221 | 59 | 37.4 | 57.2 | **19.8** | 0.48084936 |
| 2:00 PM | 897 | 0.0221 | 66.6 | 39 | 62.9 | **23.9** | 0.64577295 |
| 3:00 PM | 779 | 0.0221 | 73.1 | 37.8 | 63.7 | **25.9** | 0.80581751 |
| 4:00 PM | 681 | 0.0221 | 67.5 | 37.5 | 63.3 | **25.8** | 0.91822051 |
| 5:00 PM | - | 0.0221 | 63.7 | 36.7 | 56.7 | **20** | - |
| 6:00 PM | - | 0.0221 | 55.4 | 36 | 52.3 | **16.3** | - |
| 7:00 PM | - | 0.0221 | 49.2 | 34.7 | 47.1 | **12.4** | - |
| 8:00 PM | - | 0.0221 | 47.8 | 32.6 | 44.4 | **11.8** | - |
| **Average** | **773.25** | | **62.508333** | **36.775** | **56.716667** | **19.94166** | **0.7183460** |

The data above are been extracted by using instrument such as digital temperature sensor and pyranometer, with addition to that flow rate is been stabled by using gaming adaptor in which there were different sets of voltage ratings. The data of first day is been taken by considering mass flow rate constant as 0.02211 kg/sec, and without using **Cherry pits material**

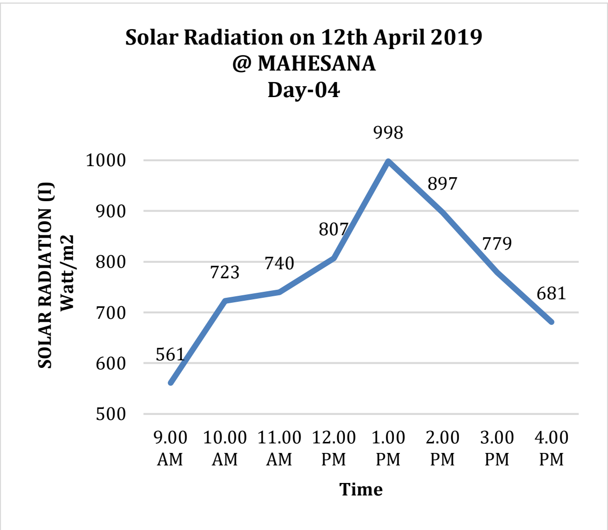


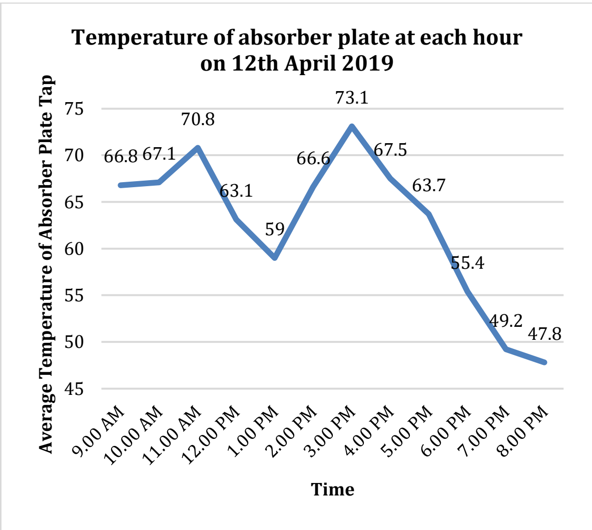

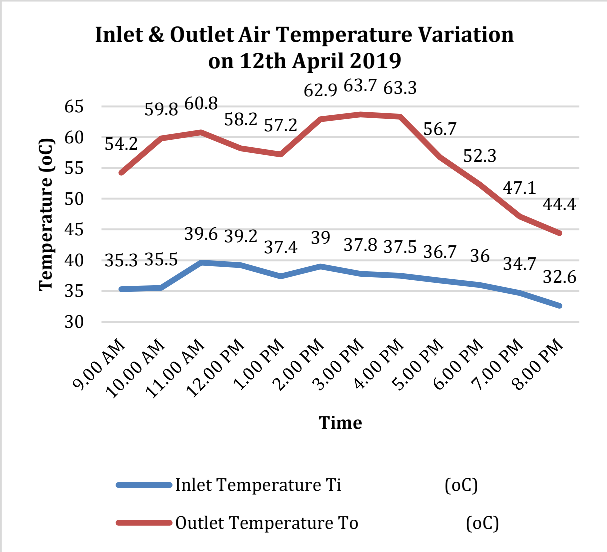


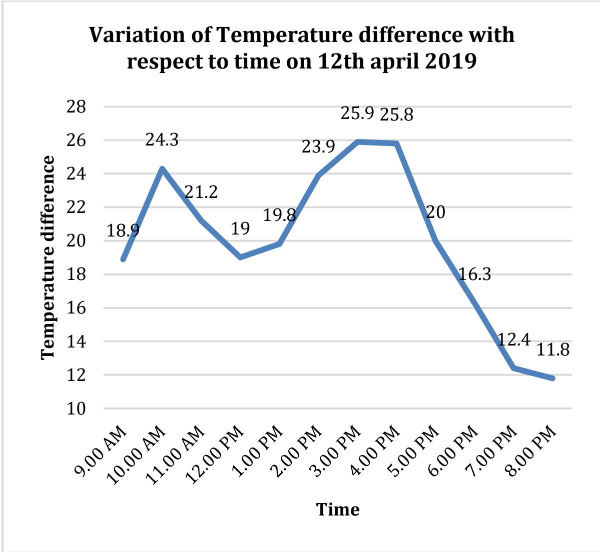


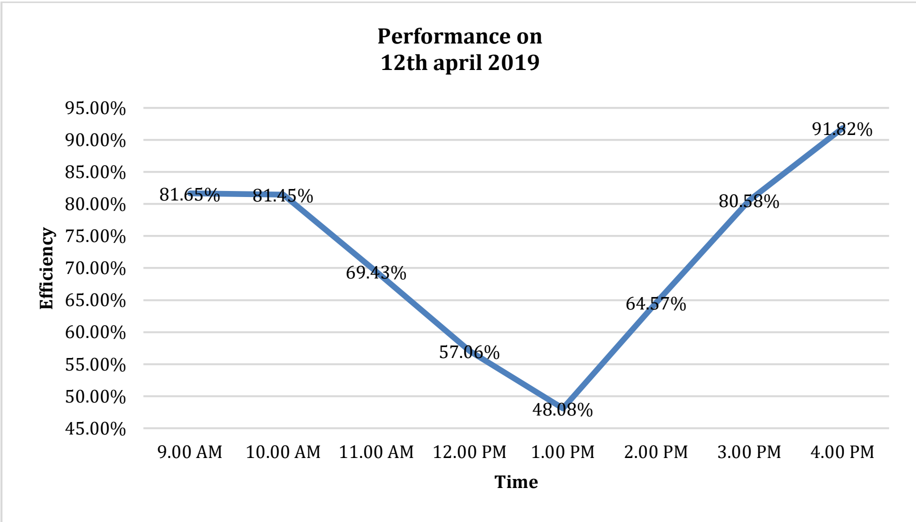


| Experimental result at different mass flow rate on **14th APRIL 2019** @ MAHESANA (LAT: 23.55 , LONG:72.35) **with Cherry pits material** | | | | | | | |
|---|---|---|---|---|---|---|---|
| **Time** | **Solar radiation (i) watt/m2** | **Mass flow rate (m) kg/sec** | **Average Temperature of Absorber Plate Tap (oC)** | **Inlet Temp. Ti (oC)** | **Outlet Temp. To (oC)** | **Temp. Difference ΔT=To-Ti (oC)** | **Efficiency = m cpΔt/I*A, cp=1004 kJ/kg.K** |
| 9:00 AM | 648 | 0.0349 | 60.9 | 31.9 | 46.8 | **14.9** | 0.87967519 |
| 10:00 AM | 745 | 0.0349 | 61.8 | 32.7 | 49.1 | **16.4** | 0.84216784 |
| 11:00 AM | 874 | 0.0349 | 63.8 | 33.9 | 49.7 | **15.8** | 0.69160278 |
| 12:00 PM | 923 | 0.0349 | 64.4 | 36 | 53 | **17** | 0.70462541 |
| 1:00 PM | 993 | 0.0349 | 65 | 36.8 | 54.7 | **17.9** | 0.68962796 |
| 2:00 PM | 1003 | 0.0349 | 65.7 | 38.2 | 58.7 | **20.5** | 0.78192303 |
| 3:00 PM | 946 | 0.0349 | 64.3 | 37.9 | 59.6 | **21.7** | 0.87756577 |
| 4:00 PM | 756 | 0.0349 | 62.8 | 37.2 | 55.9 | **18.7** | 0.94630447 |
| 5:00 PM | - | 0.0349 | 56.9 | 34.9 | 53.8 | **18.9** | - |
| 6:00 PM | - | 0.0349 | 51.8 | 34.3 | 48.6 | **14.3** | - |
| 7:00 PM | - | 0.0349 | 49.1 | 33.8 | 45.7 | **11.9** | - |
| 8:00 PM | - | 0.0349 | 47.9 | 32.6 | 42.8 | **10.2** | - |
| **Avg.** | **861** | | **59.533333** | **35.016667** | **51.533333** | **16.51666** | **0.80168656** |

The data above are being extracted by using instrument such as digital temperature sensor and pyranometer, with addition to that flow rate is been stabled by using gaming adaptor in which there were different sets of voltage ratings. The data of first day is been taken by considering mass flow rate constant as 0.02211 kg/sec, and without using **Cherry pits material**

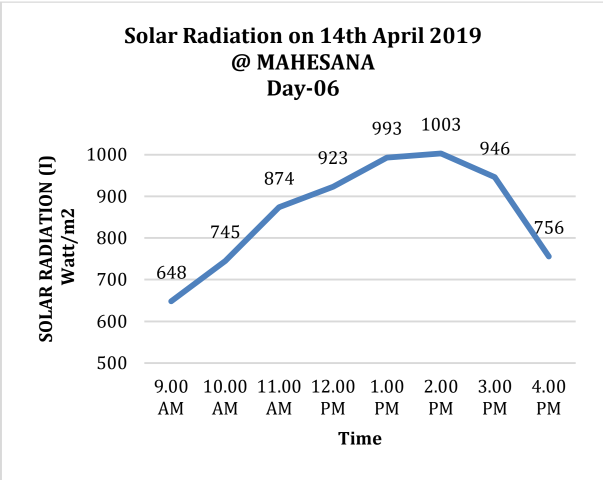


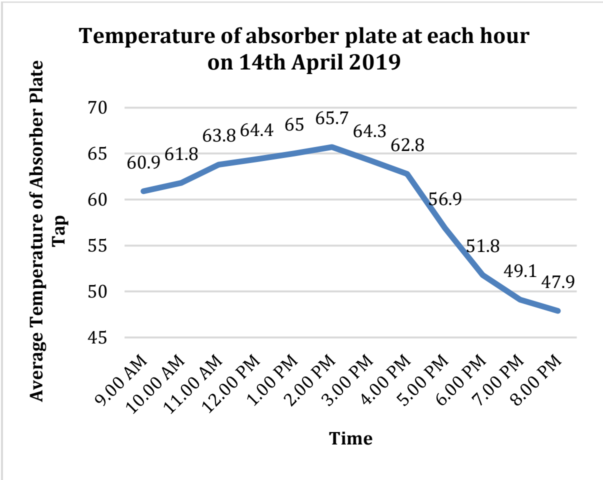


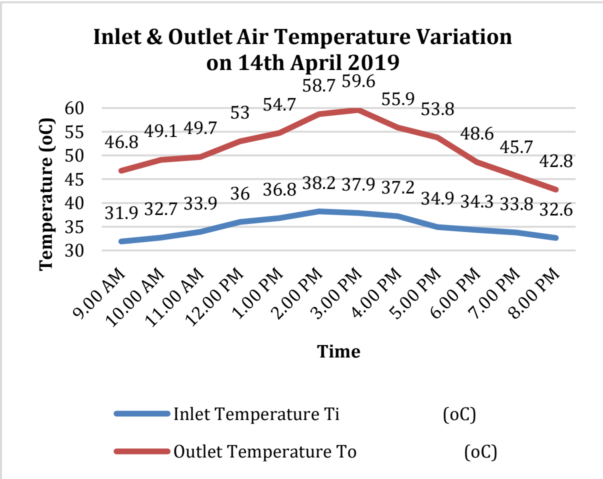


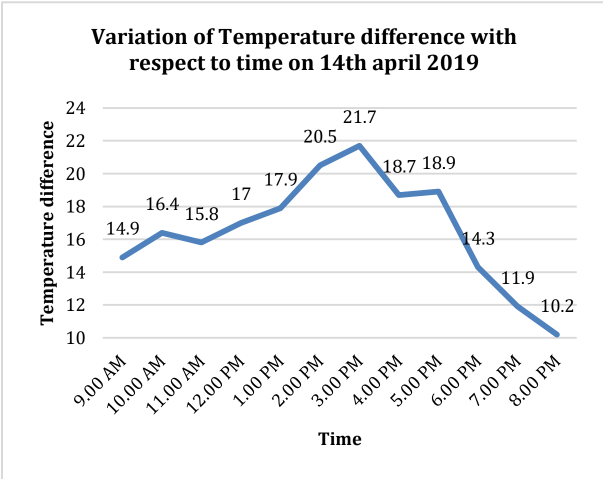


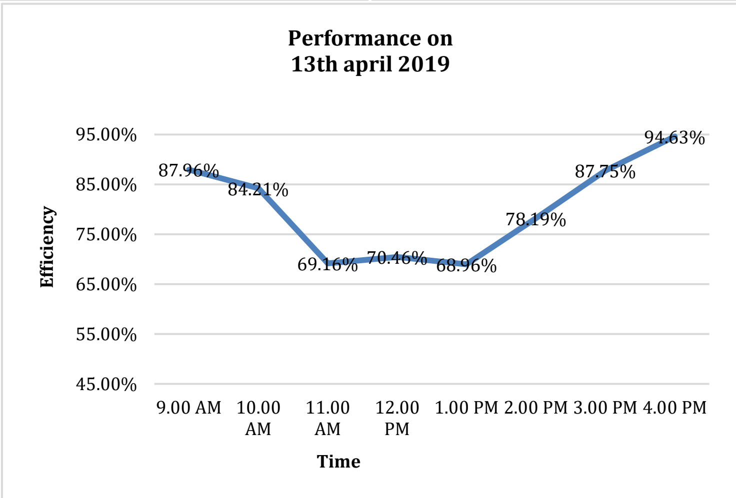


| Comparison of Solar Radiation During an Experiment | | | | | | |
|---|---|---|---|---|---|---|
| Time | 09 April 2019 | 10 April 2019 | 11 April 2019 | 12 April 2019 | 13 April 2019 | 14 April 2019 |
| 09:00 AM | 594 | 578 | 643 | 561 | 532 | 648 |
| 10:00 AM | 719 | 627 | 749 | 723 | 634 | 745 |
| 11:00 AM | 738 | 918 | 976 | 740 | 920 | 874 |
| 12:00 PM | 829 | 1008 | 938 | 807 | 1005 | 923 |
| 01:00 PM | 992 | 951 | 971 | 998 | 956 | 993 |
| 02:00 PM | 895 | 853 | 1005 | 897 | 861 | 1003 |
| 03:00 PM | 775 | 768 | 942 | 779 | 770 | 946 |
| 04:00 PM | 675 | 637 | 577 | 681 | 641 | 756 |
| 05:00 PM | 448 | 443 | 298 | - | - | - |
| 06:00 PM | 196 | 192 | 55 | - | - | - |
| 07:00 PM | 81 | 76 | - | - | - | - |
| 08:00 PM | - | - | - | - | - | - |

**Comparison of Outlet Temperature During an Experiment**

| **Time** | **09 April 2019** | **10 April 2019** | **11 April 2019** | **12 April 2019** | **13 April 2019** | **14 April 2019** |
|---|---|---|---|---|---|---|
| | **Without CPP** | **Without CPP** | **Without CPP** | **With CPP** | **With CPP** | **With CPP** |
| | **Flow Rate: 0.02211 Kg/Sec** | **Flow Rate: 0.0279 Kg/Sec** | **Flow Rate: 0.0349 Kg/Sec** | **Flow Rate: 0.02211 Kg/Sec** | **Flow Rate: 0.0279 Kg/Sec** | **Flow Rate: 0.0349 Kg/Sec** |
| **09:00 AM** | 58.7 | 45.8 | 47.8 | 54.2 | 49.7 | 46.8 |
| **10:00 AM** | 62.1 | 51.1 | 51.3 | 59.8 | 50.3 | 49.1 |
| **11:00 AM** | 62.8 | 53.2 | 57.8 | 60.8 | 51.2 | 49.7 |
| **12:00 PM** | 58.5 | 53.5 | 56.9 | 58.7 | 54.5 | 53.9 |
| **01:00 PM** | 58.8 | 55.7 | 54.8 | 57.2 | 55.2 | 55.7 |
| **02:00 PM** | 61.9 | 57.7 | 61.3 | 62.9 | 59.6 | 59.3 |
| **03:00 PM** | 63.3 | 59.2 | 60.6 | 63.7 | 57.9 | 57.8 |
| **04:00 PM** | 61.4 | 55.9 | 48.9 | 63.3 | 57.7 | 55.9 |
| **05:00 PM** | 53.9 | 50.1 | 42.4 | 56.7 | 55.7 | 53.8 |
| **06:00 PM** | 43 | 41.6 | 35.7 | 52.3 | 51.1 | 48.6 |
| **07:00 PM** | 36.7 | 36.6 | 0 | 47.1 | 45.9 | 45.7 |
| **08:00 PM** | 32.8 | 32.5 | 0 | 44.4 | 43.6 | 42.8 |

**Comparison of Temperature Variation During an Experiment**

| Time | 09 April 2019 | 10 April 2019 | 11 April 2019 | 12 April 2019 | 13 April 2019 | 14 April 2019 |
|---|---|---|---|---|---|---|
| | Without CPP | Without CPP | Without CPP | With CPP | With CPP | With CPP |
| | Flow Rate: 0.02211 Kg/Sec | Flow Rate: 0.0279 Kg/Sec | Flow Rate: 0.0349 Kg/Sec | Flow Rate: 0.02211 Kg/Sec | Flow Rate: 0.0279 Kg/Sec | Flow Rate: 0.0349 Kg/Sec |
| 09:00 AM | 23.7 | 18.2 | 15.6 | 18.9 | 16.2 | 14.9 |
| 10:00 AM | 26.6 | 16.8 | 16.1 | 24.3 | 16.5 | 16.4 |
| 11:00 AM | 23 | 18.2 | 17.5 | 21.2 | 16.4 | 15.8 |
| 12:00 PM | 19.3 | 18 | 17.6 | 19 | 17.7 | 17 |
| 01:00 PM | 21.4 | 18.9 | 18.5 | 19.8 | 18.9 | 17.9 |
| 02:00 PM | 22.9 | 19.6 | 19.5 | 23.9 | 21.3 | 20.5 |
| 03:00 PM | 25.5 | 21.8 | 21.3 | 25.9 | 22.2 | 21.7 |
| 04:00 PM | 23.9 | 18.7 | 12.2 | 25.8 | 20.5 | 18.7 |
| 05:00 PM | 17 | 13.4 | 7 | 20 | 19.3 | 18.9 |
| 06:00 PM | 7 | 5.8 | 1 | 16.3 | 15.8 | 14.3 |
| 07:00 PM | 2 | 2 | 0 | 12.4 | 12 | 11.9 |
| 08:00 PM | 0.2 | 0.1 | 0 | 11.8 | 10.9 | 10.2 |

**Comparison of Absorber Plate Temperature During an Experiment**

| Time | 09 April 2018 | 10 April 2018 | 11 April 2018 | 12 April 2018 | 13 April 2018 | 14 April 2018 |
|---|---|---|---|---|---|---|
| | Without PCM | Without PCM | Without PCM | With PCM | With PCM | With PCM |
| | Flow Rate: 0.02211 Kg/Sec | Flow Rate: 0.0279 Kg/Sec | Flow Rate: 0.0349 Kg/Sec | Flow Rate: 0.02211 Kg/Sec | Flow Rate: 0.0279 Kg/Sec | Flow Rate: 0.0349 Kg/Sec |
| 09:00 AM | 66.6 | 61.5 | 60.3 | 66.8 | 61.3 | 60.9 |
| 10:00 AM | 66.8 | 63.3 | 62.2 | 67.1 | 62.9 | 61.8 |
| 11:00 AM | 70 | 61.1 | 59.4 | 70.8 | 61.6 | 63.8 |
| 12:00 PM | 70.2 | 56.2 | 55.3 | 63.1 | 62.2 | 64.4 |
| 01:00 PM | 71.4 | 56.5 | 55.4 | 59 | 58.9 | 65 |
| 02:00 PM | 72.8 | 61.9 | 60.4 | 66.6 | 61.7 | 65.7 |
| 03:00 PM | 71.1 | 68.2 | 67.8 | 73.1 | 62.8 | 64.3 |
| 04:00 PM | 65.9 | 61.2 | 50.2 | 67.5 | 61.2 | 62.8 |
| 05:00 PM | 62.2 | 58.4 | 46.2 | 63.7 | 59.9 | 56.9 |
| 06:00 PM | 52.3 | 47.3 | 36 | 55.4 | 54.2 | 51.8 |
| 07:00 PM | 43.2 | 38.1 | | 49.2 | 49.8 | 49.1 |
| 08:00 PM | 35.1 | 32.9 | | 47.8 | 47.4 | 47.9 |

**Comparison of Performance During an Experiment**

| **Time** | **09 April 2018** | **10 April 2018** | **11 April 2018** | **12 April 2018** | **13 April 2018** | **14 April 2018** |
|---|---|---|---|---|---|---|
| | **Without PCM** | **Without PCM** | **Without PCM** | **With PCM** | **With PCM** | **With PCM** |
| | **Flow Rate: 0.02211 Kg/Sec** | **Flow Rate: 0.0279 Kg/Sec** | **Flow Rate: 0.0349 Kg/Sec** | **Flow Rate: 0.02211 Kg/Sec** | **Flow Rate: 0.0279 Kg/Sec** | **Flow Rate: 0.0349 Kg/Sec** |
| 09:00 AM | 96.70% | 96.30% | 92.81% | 81.65% | 93.13% | 87.96% |
| 10:00 AM | 89.66% | 81.94% | 82.23% | 81.45% | 79.59% | 84.21% |
| 11:00 AM | 75.53% | 60.63% | 68.59% | 69.43% | 54.51% | 69.16% |
| 12:00 PM | 56.42% | 54.61% | 71.78% | 57.06% | 53.86% | 70.46% |
| 01:00 PM | 52.28% | 60.78% | 72.88% | 48.08% | 60.46% | 68.96% |
| 02:00 PM | 62.01% | 70.27% | 74.23% | 64.57% | 75.65% | 78.19% |
| 03:00 PM | 79.74% | 86.81% | 86.50% | 80.58% | 88.17% | 87.75% |
| 04:00 PM | 85.81% | 89.78% | 80.89% | 91.82% | 97.81% | 94.63% |
| 05:00 PM | 91.96% | 92.51% | 89.86% | - | - | - |
| 06:00 PM | 86.55% | 92.38% | 69.55% | - | - | - |
| 07:00 PM | 59.84% | 80.48% | - | - | - | - |
| 08:00 PM | - | - | - | - | - | - |

| Average Values of An Experiment | | | | | | | | | |
|---|---|---|---|---|---|---|---|---|---|
| **Case** | **April 09, 2019** | **April 10, 2019** | **April 11, 2019** | **Avg without CPP** | **April 12, 2019** | **April 13, 2019** | **April 14, 2019** | **Avg With CPP** | **Final Avg** |
| | **Without CPP** | **Without CPP** | **Without CPP** | | **With CPP** | **With CPP** | **With CPP** | | |
| | **Flow Rate: 0.0221 Kg/Sec** | **Flow Rate: 0.0279 Kg/Sec** | **Flow Rate: 0.0349 Kg/Sec** | | **Flow Rate: 0.0221 Kg/Sec** | **Flow Rate: 0.0279 Kg/Sec** | **Flow Rate: 0.0349 Kg/Sec** | | |
| **Avg Solar Radiation w/m2** | 631 | 641 | 715 | **662.3** | 773.25 | 789.87 | 861 | **808.0** | **735.1** |
| **Day Avg. Temp. of Absorber Plate (oC)** | 62.3 | 55.55 | 55.32 | **57.72** | 62.5 | 58.65 | 59.53 | **60.22** | **58.97** |
| **Inlet Temp Ti (oC)** | 36.78 | 35.71 | 35.37 | **35.95** | 36.77 | 35.49 | 35.01 | **35.75** | **35.85** |
| **Outlet Temp To (oC)** | 54.49 | 50 | 50 | **51.49** | 56.71 | 52.8 | 51.53 | **53.68** | **52.58** |
| **Day Avg. Temp Diff. (oC)** | 17.7 | 14.29 | 14.63 | **15.54** | 19.94 | 17.3 | 16.51 | **17.91** | **16.72** |
| **Day Avg Efficiency (%age)** | 76.05% | 78.77% | 78.93% | **77.92%** | 71.83% | 75.4% | 80.17% | **75.8%** | **76.85%** |

Here total six number of experiment was conducted from 9 am to 8 pm every day in the month of April. The following measurement has been recorded that is air flow rate, temperature of air inside the annulus, solar radiation, ambient/atmospheric air temperature. Inlet and outlet air temperature and also wind speed. Variation for wind speed was from 0 to 3 m/s for various days and solar radiation was ranging from 40 to 1000 W/m2. And the average annual normal solar radiation for tested location (Mahesana) was found to be 5.87kwh/m2/day. The experiment was conducted for six different conditions to get the best efficiency. The measured conditions for solar air heater are tabulated in the table. Here among six experimentations first three were performed with specified mass flow rates that is 0.0221, 0.0279 & 0.0349 kg/sec, that is at a speed of 1.9m/s, 2.4 m/s & 3m/srespectively. From the data extracted from experimentation it is clear that temperature difference between inlet and outlet will increase with increase in solar radiation. From the six case area is same for all cases but the only thing that effects efficiency is mass flow rate, from the readings it is very clear that with lower mass flow rate temperature difference will be maximum but not efficiency. For optimum efficiency flow rate must be high. For last three conditions use of phase change material results in temperature rise by 2.5 degree Celsius, & reduces efficiency by 2.12%, and extends working hours by approx. 2 hours by using 05kgs of CPP. From the table it can be say that for day-01 at Day Average solar intensity 632 W/m2, and air mass flow rate of 0.0221kg/sec, the maximum temperature difference was about 17.7 degree Celsius for vertical type solar air heater without CPP, average temperature of absorber plate was 63.3°C & with day average efficiency of 76.05%. day-02 at Day Average solar intensity 641W/m2, and air mass flow rate of 0.0279kg/sec, the maximum temperature difference was about 14.29 degree Celsius for vertical type solar air heater without CPP, average temperature of absorber plate was 56.5°C & with day average efficiency of 78.7%. day-03 at Day Average solar intensity 715W/m2, and air mass flow rate of 0.035kg/sec, the maximum temperature difference was about 14.63 degree Celsius for vertical type solar air heater without PCM, average temperature of absorber plate was 55.32°C & with day average efficiency of 79.93%. day-04 at Day Average solar intensity 776.2W/m2, and air mass flow rate of 0.0221kg/sec, the maximum temperature difference was about 19.94degree Celsius for vertical type solar air heater with PCM, average temperature of absorber plate was 62.6°C & with day average efficiency of 71.83%. day-05 at Day Average solar intensity 789.8W/m2, and air mass flow rate of 0.0279kg/sec, the maximum temperature difference was about 17.3 degree Celsius for vertical type solar air heater with CPP, average temperature of absorber plate was 58.75°C & with day average efficiency of 75.6%. day-06 at Day Average solar intensity 861W/m2, and air mass flow rate of 0.0348kg/sec, the maximum temperature difference was about 16.51degree Celsius for vertical type solar air heater with CPP, average temperature of absorber plate was 59.53°C & with day average efficiency of 80.17%. From the graph we can see the variations of the hourly temperature difference of air for specified three mass flow rates with and without using CPP. We can observe from graph that from 9 am to 1 pm, temperature of thecomplete assembly increases, after that temperature of air is reducing. According to most of the cases temperature difference of flowing air is maximum between 12pm to 2 pm,that is because of maximum solar radiation available. We can also observe that temperature difference is higher with low air flow rate and lower with high air flowing rate. But efficiency is lower with low air flow rate and higher with high air flow rate. It means we need to set our parameter as our requirement. The energy loss by heat transferred to fluid will increase if we increase mass flow rate of air because high Reynolds number will increase the intensity of turbulent flow that will help to enhance better heat transfer to air. Here highest average efficiency was 80.17% that was achieved by experimental setup for day-6, and if we consider working hours as well than experimental setup day-4 is best, since it gives additional 2 hours for working.

## Conclusion

The experimental evaluation of solar air heater with finned vertical absorber was done at Mahesana, Gujarat. And I come on the conclusion that changing the traditional concept with flat plate and eliminating insulation from it is definitely changes the performance. The result indicates that the highest efficiency was achieved for setup no-6, and that is 80.17 %, for flow rate of 0.0349 kg/s, and day average solar irradiation of 808 W/m2. And with the mass flow rate of 0.0221 kg/s and usage of 05 kg CPP will lead to give time rise around 2 hours. More research may be carried out by altering number of fins, increasing height of absorber plate and area, or by modifying to multi-pass system for air flow.

## References


S.S. Krishnananth, K. KalidasaMurugavel *et al.* (2018) Experimental study on double pass solar air heater with thermal energy storage.

MesutAbuşka, SeyfiŞevik *et al.* (2018) Experimental performance analysis of sensible heat storage in solar air collector with cherry powder under the natural convection

Aldabbagh, L. B. Y., F. Egelioglu, and M. Ilkan. "Single and double pass solar air heaters with wire mesh as packing bed." Energy 35.9 (2010): 3783-3787.

Krishnananth, S. S., and K. KalidasaMurugavel. "Experimental study on double pass solar air heater with thermal energy storage." Journal of King Saud University Engineering Sciences 25.2 (2013): 135-140.

Abdallah, Salah, Mazen M. Abu-Khader, and Omar Badran. "Effect of various absorbing materials on the thermal performance of solar stills."Desalination 242.1 (2009): 128-137.

RahelehNowzari ,L.B.Y. Aldabbagh , F. Egelioglu "Single and double pass solar air heater with partially perforated cover and packed mesh" Energy 73 (2014) 694-702.

PaisarnNaphon"Effect of porous media on the performance of the double pass flat plate solar air heater" International Communications in Heat & Mass transfer 32 (2005) 140-150

Saravanakumar, P. T., K. Mayilsamy, and M. Mohanraj. "Numerical study and thermal performance of the flat plate solar air heaters with and without thermal storage." (2006).

Esen, Hikmet. "Experimental energy and exergy analysis of a double-flow solar air heater having different obstacles on absorber plates." Building and Environment 43.6 (2008): 1046-1054.

Mahmood, A. J., L. B. Y. Aldabbagh, and F. Egelioglu. "Investigation of single and double pass solar air heater with transverse fins and a package wire mesh layer." Energy Conversion and Management 89 (2015): 599-607.

Chii-Dong Ho, Hsuan Chang-Sheng Lin, Chun-Chieh Chao and Yi-En "Analytical and experimental studies of wire packed double-pass solar air heaters under recycling operation" Energy Procedia 75 (2015) 403-409.

K.Mohammadi, M. Sabzpooshani, "Comprehensive performance evaluation and parametric studies of single pass solar air heater with fins and baffles attached over the absorber plate" Energy 57 (2013) 741-750.

Yang, Ming, *et al.* "Design and optimization of a solar air heater with offset strip fin absorber plate." Applied Energy 113 (2014): 1349-1362.

Badache, Messaoud, StéphaneHallé, and Daniel Rousse. "A full 3 4 factorial experimental design for efficiency optimization of an unglazed transpired solar collector prototype." Solar Energy 86.9 (2012): 2802-2810.

Chamoli, Sunil. "ANN and RSM approach for modeling and optimization of designing parameters for a V down perforated baffle roughened rectangular channel." Alexandria Engineering Journal 54.3 (2015): 429-446.

Singh, Nikhil, and Vishal Francis. "Investigating the Effect of Water Temperature and Inclination Angle on the Performance of Single Slope Solar Still: A Taguchi Approach."

Morimoto, T., *et al.* "Optimization of heat treatment for fruit during storage using neural networks and genetic algorithms." Computers and Electronics in Agriculture 19.1 (1997): 87-101.

Kassem, Abd El-Wahab S., Al-Sulaiman, Mohammed A. "Predicting Drying Efficiency during Solar Drying Process of Grapes Clusters in a Box Dryer using Artificial Neural Network." Australian Journal of Basic & Applied Sciences;2011, Vol. 5 Issue 6, p230

Jadhav, Deepak Baburao, *et al.* "Solar cabinet drying of bitter gourd: Optimization of pretreatments and quality evaluation." International Journal of Food Engineering 6.4 (2010).

Medugu, D. W. "Performance study of two designs of solar dryers." Arch. Appl. Sci. Res 2.2 (2010): 136-148

Vijay Singh Bisht at al."Review and performance evaluation of roughened solar air heatersSci. Res 2.2 (2018):

Anil Kumar at al."Experimental Study on the Performance of Double Pass and Two Inlet Ports Solar Air Heater (SAH) at Different Configurations of the Absorber PlateSci. Res 3.2 (2017)